Grid Frequency Control Capability of Energy Storage Systems: Modeling, New Control Approach, and Real-time Validation

Oshnoei, Arman; Oshnoei, Soroush; Jalilpoor, Kamran; Soudjani, Sadegh; Blaabjerg, Frede

Published in:
The 8th IEEE Workshop on the Electronic Grid (eGrid 2023)

Publication date:
2023

Grid Frequency Control Capability of Energy Storage Systems: Modeling, New Control Approach, and Real-time Validation

Arman Oshnoei
Department of energy
Aalborg University
Aalborg, Denmark
aros@energy.aau.dk

Soroush Oshnoei
Department of Electrical and Computer Engineering
Aarhus University
Aarhus, Denmark
soroush_oshnoei@yahoo.com

Kamran Jalilpoor
Department of Electromechanical, Systems and Metal Engineering
Ghent University
Ghent, Belgium
Kamran.jalilpoor@UGent.be

Sadegh Soudjani
School of Computing
Newcastle University
Newcastle, United Kingdom
Sadegh.Soudjani@newcastle.ac.uk

Frede Blaabjerg
Department of energy
Aalborg University
Aalborg, Denmark
fbl@energy.aau.dk

***Abstract*—Energy storage systems (ESSs) have proved to be efficient in frequency regulation by providing flexible charging/discharging powers. This paper presents a model predictive control (MPC) with feedback correction (FC) to provide the ESS with control signals to be efficiently involved in the frequency regulation in a power system with renewable power generation. The FD is introduced to improve the accuracy of the prediction in the MPC. An approach based on the artificial neural network (ANN) is presented for optimal design of the weighting coefficients appearing in the MPC objective function. The controller performance is compared with an MPC without feedback correction, a fuzzy-PD control, and a scheme with no support from the ESS. A comparison is also made to examine the effect of weighting coefficients tuned by the ANN with those tuned by a fuzzy intelligent method and a sine-cosine algorithm. Real-time validations are provided to demonstrate the proposed method's effectiveness.**

***Index Terms*—Energy storage system, Artificial neural network, load frequency control, model predictive control.**

I. Introduction

Renewable Energy Sources (RESs) have been consistently advancing globally to tackle energy deficits and promote low-carbon initiatives. The RESs such as the photovoltaic and wind generations, are largely dependent on environmental conditions and exhibit intermittent and uncertain behavior. Integrating these generations can, therefore, raise severe stability concerns, including frequency regulation issues [1, 2]. Consequently, more operating reserves and complex control methods will be required in power systems with high integration of RESs. Energy Storage Systems (ESSs) offer promising solutions for providing such additional reserves. Due to the quick response and high ramp rate, the ESS can improve the controllability of the system and provide energy management solutions [3]. The utility grid commonly owns large-scale ESSs and offers capacities of up to tens of MWh in a few facilities. On the other hand, small-scale ESSs are distributed throughout the power systems. The small-scale ESSs commonly offer capacities up to hundreds of kWh in many facilities. The distributed ESSs located at the demand side are, however, usually more extensive in number but more minor in capacity. Hence, their individual contributions to the network are relatively minimal [4].

The ESSs can provide ancillary services, including frequency and voltage regulation, through controlled discharging/charging of power to/from the system. Nowadays, this appears as the main function of utility-scale batteries. The ESS provides primary frequency regulation reserves in [5] and [6]. The State of Charge (SoC) limit appears as a severe constraint of the actual applications of ESS [7]. In [8], a comprehensive review is provided for the participation of the ESS in frequency regulation regarding design considerations, connection requirements, and real implementation. A load frequency control (LFC) strategy is suggested in [9] based on the droop control and SoC feedback to make coordination between the ESS and the conventional unit. A control scheme is developed in [10] based on adaptive dynamic programming to use ESS during frequency excursion events efficiently. A finite-time consensus method is also used in [11] to generate the control commands for the ESSs participating in the regulation service. A centralized, coordinated control for ESSs and heat pump water heaters participating in LFC is presented in [12]. The stability considerations associated with the time delay caused by the propagation channels in the ESS control have garnered minimal focus in the published research.. The

This work was supported by the Reliable Power Electronic-Based Power Systems (REPEPS) project at the AAU Energy Department, Aalborg University, as a part of the Villum Investigator Program funded by the Villum Foundation.

sensitivity of the frequency response to the ESS contribution in LFC also received little attention. Model Predictive Control (MPC), as a far-reaching methodology in controlling modern power systems, is primarily used in LFC studies [13]. The MPC is suggested in [14] to enhance the frequency response of a microgrid with electric vehicles serving as storage appliances. A robust MPC is presented in [15] to control the distributed ESSs in a system with uncertain wind generations. Although these studies prioritize the development of prediction models, cost functions, and computational efficiency to achieve satisfactory performance for a wide range of applications, they tend to overlook the impact of model mismatches. Hence, a modeling error compensation method is required in the MPC structure to compensate for prediction error, which is addressed in this paper.

This paper proposes a control method based on the MPC with feedback correction to adjust the ESS output power in an isolated power system. The frequency dynamics are obtained in an isolated power system with ESS to calculate the closed-loop and open-loop transfer functions. A feedback correction is designed to be included with the MPC in the ESS control loop to improve the MPC prediction accuracy and create disturbance rejection ability in the MPC structure. An intelligent method based on the Artificial Neural Network (ANN) learning features is used to obtain optimal weighting coefficients for the MPC with feedback correction. The controller performance is evaluated by comparing it to various other control schemes. These include an MPC without feedback correction, a fuzzy-PD control, and a scheme that does not utilize the support of the ESS. Additionally, a comparison is conducted to analyze the impact of the weighting coefficients tuned by an ANN in contrast to those tuned by a fuzzy intelligent method and a sine-cosine algorithm.

II. System Modeling

The bidirectional power exchange capability of the ESS makes it an efficient back-up for the frequency support. The control center of ESS submits the ESS capacity available for the frequency regulation to the transmission system operator. Based on the frequency deviation and the available capacity, the operator provides the control center with a dispatch command. The control center subsequently issues a regulation signal to the ESS. In response to this control instruction, the ESS charges or discharges power to or from the system, but only if the frequency deviation surpasses a dead zone defined by a positive upper limit and a negative lower threshold. The schematic representation of the ESS control used for frequency regulation can be seen in Fig. 1. As can be seen, the ESS control includes two functional parts of primary and secondary controls.

The ESS is assumed to be connected to an isolated power system. The system comprises a reheated thermal generator, a renewable energy production, an ESS unit together with the load demand. The production of the wind farm as the renewable unit is assumed to be the source of uncertainty

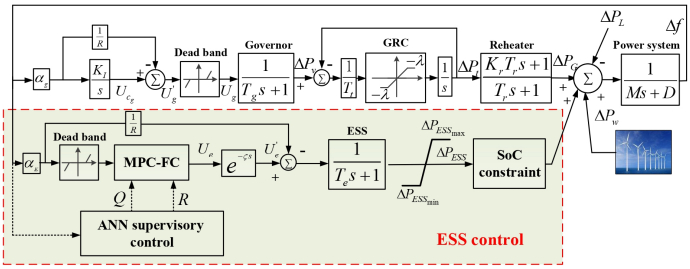

Fig. 1. Frequency response model of the isolated power grid.

in the system. The dynamics of frequency deviation can be characterized by the subsequent differential equation:

$$\frac{\mathrm{d}(\Delta f)}{\mathrm{d}t} = -\frac{D}{M}\Delta f + \frac{1}{M}\left(\Delta P_G + \Delta P_w + \Delta P_{ESS} - \Delta P_L\right), \tag{1}$$

where ΔP_G, ΔP_w, ΔP_{ESS}, and ΔP_L represent the variation in the output power of the thermal generator, wind farm, ESS, and in load value, respectively; M is the inertia constant of the thermal generator; and D represents the load damping coefficient. The injected power of the ESS is assumed to be positive when the ESS is in discharging mode and negative when in charging mode. The nonlinear feature pertaining to the Governor Dead Band (GDB) is integrated into the model and can be represented as:

$$U_g(t) = \max(0, U'_g - U'_{g0}) + \min(0, U'_g + U'_{g0}) \tag{2}$$

where the operators *max* and *min* yield the largest and smallest values among their inputs, respectively; $\pm U'_{g_0}$ define the limits of the dead zone; and U'_g is the signal designated for the governor, computed as:

$$U'_g = U_{c_g} - \frac{\Delta f}{R} \tag{3}$$

where U_{c_g} represents the signal generated by the controller, and R is the speed regulation coefficient. The coefficients α_G and α_E are distribution coefficients for the contribution of the generator and the ESS unit in frequency regulation, respectively. The coefficients add up to unity. The effect of the Generation Rate Constraint (GRC) on turbine power can be represented with the following model:

$$P_t = \int [\min\left(\max(0, \frac{\mathrm{d}P'_t}{\mathrm{d}t}), \lambda\right) + \max\left(\min(0, \frac{\mathrm{d}P'_t}{\mathrm{d}t}), -\lambda\right)]\mathrm{d}t \tag{4}$$

where P'_t is the input signal directed to the GRC block, and $\pm\lambda$ establish the upper and lower permissible values for the generation rate.

It should be noted that the steady-state deviation in the ESS power will ultimately dissipate. This indicates that as system frequency is restored, the steady-state deviation in the ESS power converges to zero. In other words, when the frequency deviation returns to zero, the embedded controller removes the ESS from the regulation mechanism. Subsequently, the generator takes on the role of responding to steady-state load variations.

III. Design of Model Predictive Control with Feedback Correction for ESS

A. Overall Description

MPC is a type of closed-loop optimal control method over a finite time horizon. The controller produces control signals at a sampling interval T_s by optimizing a cost function, which encompasses the system model and both the present and past system signals. MPC provides the dual advantage of integrating an optimization process and managing constraints. In this paper, the constraints range from device-specific limitations like ESS output power to broader system restrictions such as permissible frequency deviation. The proposed MPC is segmented into three components: rolling optimization, predictive modeling, and feedback adjustment.

B. Prediction Model and Feedback Correction

The ESS's frequency deviation signal can be discretized from equation (1) employing the first-order Euler discretization, as detailed at the beginning of Page 4, where $\Delta f(k+1|k)$ is the frequency deviation at sample $k+1$ provided that it is preceded by sample k. As figured out earlier, the ESS is supplied with a fraction of the frequency deviation Δf as follows:

$$\Delta f_{ESS}(k+1|k) = \alpha_E \Delta f(k+1|k) \tag{6}$$

Due to diverse issues, the actual value of Δf_{ESS} may differ from the predicted signal. In order to have an improved prediction accuracy, a feedback correction is proposed to modify the predicted value of frequency deviation as follows:

$$\Delta f_{ESS,m}(k+1|k) = \Delta f_{ESS}(k+1|k) + P(k) \tag{7}$$

where $P(k)$ represents a correction term, which is given as follows:

$$P(k) = \gamma \left[\Delta f_{ESS}(k) - \Delta f_{ESS,m}(k|k-1)\right] \tag{8}$$

where γ is the correction factor. A too small or too large correction factor will give rise to a poor prediction of Δf_{ESS}. The correction factor in this paper is considered equal to 0.2.

C. Rolling Optimization

The MPC is furnished with the observed value of $\Delta f_{ESS,m}$. It then imparts the control signal U_e to the system model such that the resultant output closely approximates the reference output Δf^*_{ESS} , all while ensuring minimized control effort. The generation of the control signal is designed to optimize the subsequent objective function:

$$P(k) = Q\left[\Delta f_{ESS,m}(k+1|k) - \Delta f^*_{ESS}(k+1)\right]^2 + RU_e^2(k) \tag{9}$$

where Q and R serve as the weighting coefficients for the MPC's input and output, respectively. The reference output Δf^*_{ESS} is set to zero. At time $k+1$, the optimization procedure is iterated using the principal data from time k. The comprehensive MPC control framework for the ESS system is depicted in Fig. 2.

As pointed out, the control signal is required to satisfy physical and operational constraints as follows:

$$\begin{aligned} \Delta f_{ESS_{min}} \leq & \Delta f_{ESS} \leq \Delta f_{ESS_{max}} \\ U_{e_{min}} \leq & U_e \leq U_{e_{max}} \\ \Delta P_{ESS_{min}} \leq & \Delta P_{ESS} \leq \Delta P_{ESS_{max}}. \end{aligned} \tag{10}$$

The constraint associated with the SoC should be taken in consideration in producing the control commands. The ESS charge and discharge cause the SoC to vary as follows:

$$SoC(t) = \begin{cases} SoC_0 - \int P_c(t)\mathrm{d}t & \text{if } SoC_{min} < SoC(t) < SoC_{max} \\ SoC_0 - \int P_c(t)\mathrm{d}t & \text{if } SoC(t) = SoC_{max}, P_c(t) > 0 \\ SoC_0 - \int P_c(t)\mathrm{d}t & \text{if } SoC(t) = SoC_{min}, P_c(t) < 0 \\ SoC_0 & \text{otherwise} \end{cases} \tag{11}$$

where SoC_0, SoC_{min}, and SoC_{max} denote the initial SoC, and the minimum and maximum allowed values of SoC, respectively; and $P_c(t)$ represents the ESS charging/discharging power, which is expressed as follows:

$$P_c(t) = \begin{cases} P_{ESS}(t)/\beta & \text{if } 0 \leq P_{ESS}(t) \leq P_{ESS_{max}} \\ \beta P_{ESS}(t) & \text{if } P_{ESS_{min}} < P_{ESS}(t) \leq 0 \end{cases} \tag{12}$$

where β represents the charging-discharging efficiency.

IV. Intelligent Tuning of MPC Weighting Factors

The performance of an MPC is highly influenced by the magnitude of the weighting coefficients. An ANN-based methodology is proposed in this paper for optimal tuning of the weighting coefficient appearing in (9). The schematic of the ANN supervisory control for optimal tuning of the MPC weights is shown in Fig. 3. Three main steps are depicted in the figure. In the first step, the Root Mean Square (RMS) of the frequency deviation and its derivative are computed for each combination of the inputs Q and R. The weighting coefficients are chosen from 0 to 5 with an interval step of 0.5, thus 11 values for each weighting coefficient and 121 combinations of weighting coefficients. This range is chosen to sweep the combinations that give a satisfactory operation conditions. The RMS of the frequency deviation and its derivative can be simply obtained from power system dynamics model results described in Fig. 1. The trained ANN can provide accurate estimations of frequency deviation and its derivative for the given Q and R combinations. It is to be noted that the first two steps are conducted only once for a given ESS topology and given operating conditions. The learning procedure deals with the minimization of the mean squared error as follows:

$$\min \frac{1}{2}\left(\Delta f_{rms} - \Delta f_{rms,d}\right)^2 + \frac{1}{2}\left(\Delta f'_{rms} - \Delta f'_{rms,d}\right)^2 \tag{13}$$

where Δf_{rms} and $\Delta f'_{rms}$ refer to the RMS of the frequency deviation and its derivative, and $\Delta f_{rms,d}$ and $\Delta f'_{rms,d}$ are the corresponding RMSs for the training data. After completing the learning process, in the final step, the obtained ANN is used to evaluate the cost function so as to identify the optimal weighting coefficients. The cost function is defined as the RMS of the frequency deviation over the simulation period. As

$$\Delta f(k+1|k) = \left(1 - \frac{DT_s}{M}\right)\Delta f(k) + \frac{T_s}{M}\left(\Delta P_G(k) + \Delta P_{ESS}(k) + \Delta P_w(k) - \Delta P_L(k)\right) \quad (5)$$

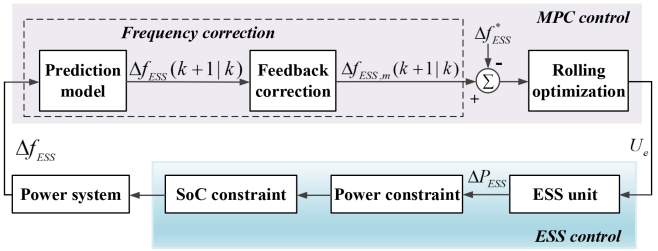

Fig. 2. Block diagram of the proposed MPC-FC for the ESS.

TABLE I
GENERATOR PARAMETERS

Parameters	Value	Parameter	Value
T_g	0.08s	M	0.1667 pu MW/Hz
T_t	0.3s	D	0.0084 pu MW/Hz
T_r	10s	R	5.6 Hz/pu MW
K_r	0.5	B	0.425 pu MW/Hz
K_I	-0.033		

the figure implies, the designed ANN comprises two neurons in the input layer corresponding to the parameters Q and R, five neurons in the hidden layer, and two neurons in the output layer corresponding to the two performance indices the frequency deviation and its derivative. The weights of the ANN are updated based on the supervised feedback approach in which the back-propagation algorithm is used for the learning procedure [16].

V. SIMULATION RESULTS AND DISCUSSIONS

The simulation studies are conducted on an isolated power system. The generator and ESS parameters are shown in Tables I and II, respectively. The generation rate of governor is assumed to be constrained by rising/falling slew rates of 10% per minute (0.0017 p.u. MW/s). A wind farm is assumed to be connected to the system. The variation of the wind farm generation is shown in Fig. 4. The frequency deviation is distributed between the generator and ESS using distribution coefficients of 0.7 and 0.3, respectively. The upper and lower bounds of the dead zone for the ESS are assumed to be ± 0.003 Hz. In the design process of the MPC, the prediction and control horizons are assumed equal to 10 and 3, respectively, with a sampling interval time of 0.1 s. The suggested LFC system is evaluated using the OPAL-RT real-time (RT) simulator. The power grid model created in MATLAB/SIMULINK is compiled with RT-LAB software to translate the model to C language for the RT simulation. Fig. 5 shows the real-time experimental setup.

A. Dynamic performance of the proposed control strategy

The efficacy of the ESS control method is assessed by initiating a step load increase of 15 MW at $t = 5$ s, succeeded by a 10 MW load reduction at $t = 50$ s. Fig. 6 displays the associated frequency fluctuations. The results include the frequency responses associated with the MPC with feedback correction, a conventional MPC, a fuzzy-PD control, and a scheme with no support from the ESS. The fuzzy controller is provided with Δf_{ESS} and its derivative. A PD controller is employed to provide the ESS with control commands. The parameters of the PD controller are tuned online during the disturbance by using the designed fuzzy controller. As the results imply, without the ESS, for a 0.015 pu load change at 5 s, Δf will reach -0.143 Hz, whereas with the ESS, with all the controllers examined, the frequency deviation remains below -0.13 Hz and below -0.1 Hz by using the MPC-FC, which demonstrates the superior performance of the MPC-FC in comparison to the other ones. The regulating power provided by the generator and by the ESS with the examined methods are shown in Figs. 7 and 8, respectively.

TABLE II
ESS PARAMETERS

Parameter	Value	Parameter	Value
SoC_0	65%	$\Delta P_{ESS_{max}}$	0.01 pu
SoC_{min}	30%	$\Delta P_{ESS_{min}}$	-0.01 pu
SoC_{max}	90%	Q_{ESS}	25 kWh
T_e	0.5s	β	0.9

When the load increases and the ESS perceives a frequency deviation signal surpassing the established dead-bands, it raises its output power by curtailing its charging capacity. In each controller considered, the ESS's power increase is notably sharper compared to that of the generator. As the system frequency realigns, the regulating power of the ESS demonstrates a decremental trajectory, settling eventually at zero. The graphical representation highlights the promptness of the ESS's response; facilitated by the proposed controller, it enables greater power interchange with the grid, hence emphasizing the mitigation of frequency deviation. Due to the sufficient reserve capacity that the generator offers, the ESS mainly contributes to the regulation service in the first seconds, and phases out with the power system recovering to the steady state. Fig. 9 illustrates the SoC fluctuations under the use of the proposed MPC-FC controller. The ESS's engagement in frequency regulation is ensured, given the SoC remains within prescribed boundaries.

B. Efficiency of the proposed ANN-based fine tuner approach

Error assessment metrics are detailed and displayed in Table III to compare the proposed ANN-based MPC-FC with MPC-FC methods tuned by fuzzy intelligent method and by a sine-cosine algorithm. These criteria are the root mean square value of deviation, the absolute maximum deviation, and

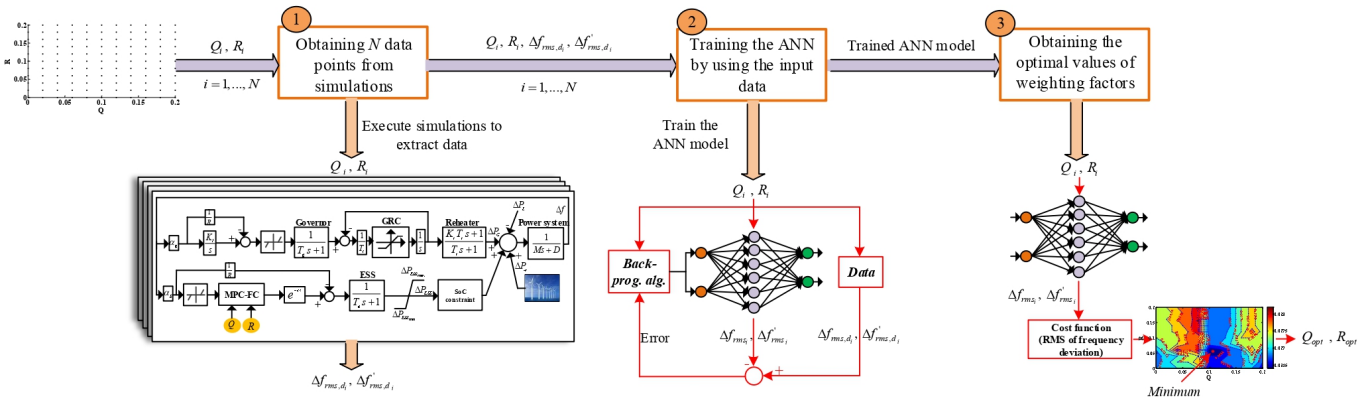

Fig. 3. Proposed ANN structure for tuning weighting coefficients.

TABLE III
PERFORMANCE INDICES BY USING ANN PREDICTION, FUZZY LOGIC, AND SINE-COSINE ALGORITHM

3*Tuning method	Δf		
	Absolute maximum deviations (Hz)	RMS value of deviations (Hz)	|ROCOF|(Hz/s)
Sine cosine algorithm [15]	0.1556	0.0425	0.1352
Fuzzy logic	0.1297	0.0354	0.1127
ANN prediction	0.1037	0.0283	0.0901

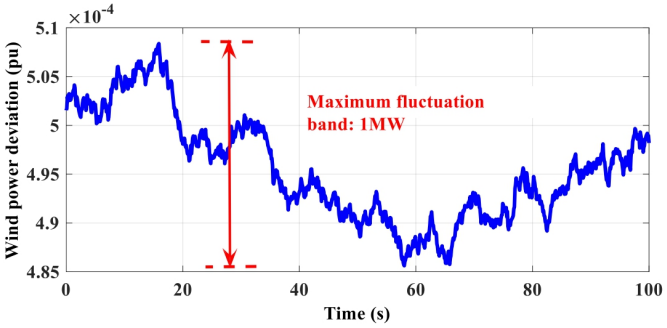

Fig. 4. Fluctuation in wind farm power.

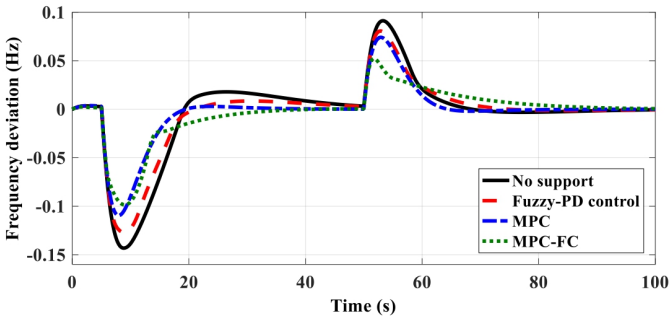

Fig. 6. Frequency response with various control methods.

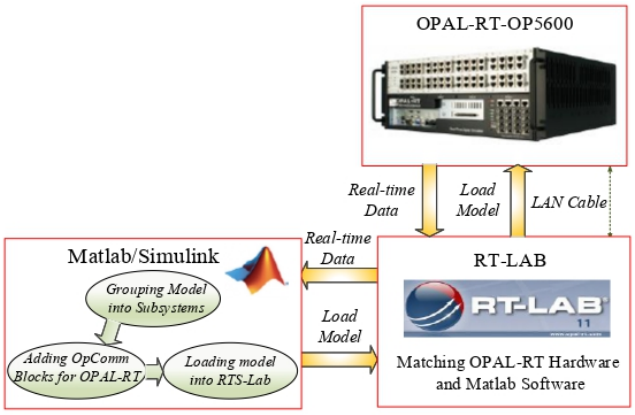

Fig. 5. Real-time experimental setup.

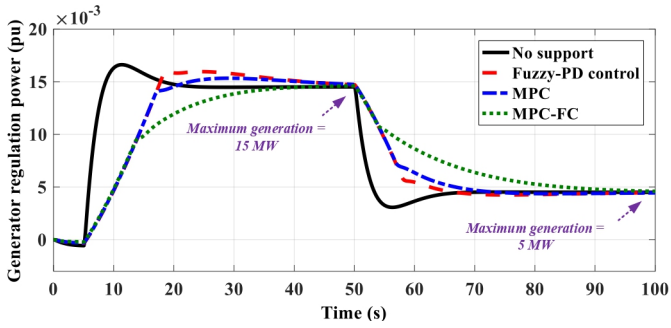

Fig. 7. Generator output power.

ROCOF. As indicated by the table, the ANN prediction method yields the lowest values in the given error criteria. Figure 10 shows the plot of the cost function (colored bars) for various combinations of weighting coefficients. The optimal weighting coefficients are obtained equal to $Q = 2.7$ and $R = 1.26$. The simulation with the obtained weighting coefficients results in

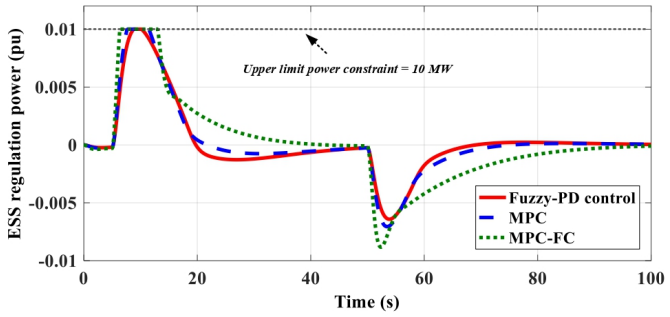

Fig. 8. ESS Regulating power.

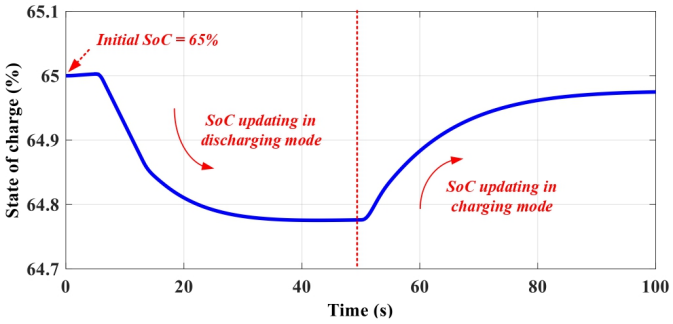

Fig. 9. Variation in the SOC of ESS with the proposed controller.

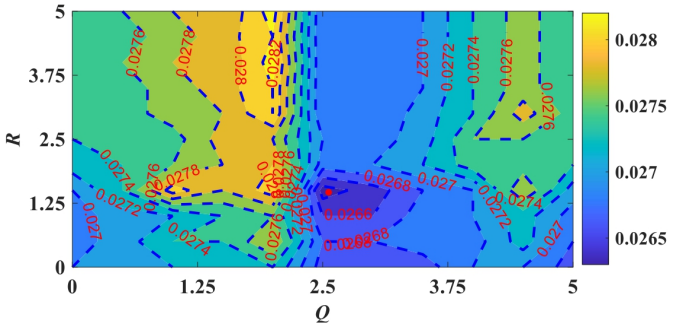

Fig. 10. Cost function in (13) for various combinations of weighting coefficients.

an RMS of 0.0265 Hz, which is indicated by a red dot. The figure also indicates that an increased weighting coefficient R with the weighting coefficient Q between 1.25 and 2.4 gives rise to poor cost function values (yellow colored).

VI. Conclusion

In this paper, a model predictive control approach with feedback correction is proposed to regulate the ESS charging/discharging power to participate in the frequency regulation of an isolated power system. A model is developed to deal with the uncertainties introduced by the wind power generation and loads, and the capability of the presented feedback-correction control is demonstrated in providing an improved frequency deviation prediction with the concerned uncertainties. The findings suggest that the suggested approach produces more efficient charging/discharging commands in comparison to the other methods examined. The method also proves efficient in satisfying the constraint in the maximum deliverable power by the ESS. The results also indicate that the ESS output power rises more steeply than the generator power. It is illustrated that the steady state ESS power vanishes with the recovery of system frequency. An ANN supervisory method is developed for tuning the MPC weighting coefficients. The results demonstrate that tuning the weighting coefficients by the ANN offers advantages over the fuzzy logic and the sine-cosine algorithm.

References

[1] T. Zhao and Z. Ding, "Cooperative optimal control of battery energy storage system under wind uncertainties in a microgrid," *IEEE Trans. Power Syst.*, vol. 33, no. 2, pp. 2292–2300, 2017.

[2] A. Oshnoei, O. Sadeghian, and A. Anvari-Moghaddam, "Intelligent Power Control of Inverter Air Conditioners in Power Systems: A Brain Emotional Learning-Based Approach," *IEEE Transactions on Power Systems*, pp. 1–15, 2022, doi: 10.1109/TPWRS.2022.3218589.

[3] G. He et al. "Cooperation of wind power and battery storage to provide frequency regulation in power markets," *IEEE Trans. Power Syst.*, vol. 32, no. 5, pp. 3559–3568, 2016.

[4] S. Vazquez, S. M. Lukic, E. Galvan, L. G. Franquelo, and J. M. Carrasco, "Energy storage systems for transport and grid applications," *IEEE Trans. Ind. Electron.*, vol. 57, no. 12, pp. 3881–3895, 2010.

[5] X. Feng, H. B. Gooi, and S. X. Chen, "Hybrid energy storage with multimode fuzzy power allocator for PV systems," *IEEE Trans. Sustain. Energy.*, vol. 5, no. 2, pp. 389–397, Apr. 2014.

[6] A. Oudalov, D. Chartouni, and C. Ohler, "Optimizing a battery energy storage system for primary frequency control," *IEEE Trans. Power Syst.*, vol. 22, no. 3, pp. 1259–1266, 2007.

[7] P. Mercier, R. Cherkaoui, and A. Oudalov, "Optimizing a battery energy storage system for frequency control application in an isolated power system," *IEEE Trans. Power Syst.*, vol. 24, no. 3, pp. 1469–1477, 2009.

[8] L. Meng, J. Zafar, S. K. Khadem, A. Collinson, K. C. Murchie, F. Coffele, and G. Burt, "Fast Frequency Response from Energy Storage Systems-A Review of Grid Standards, Projects and Technical Issues," *IEEE Trans. Smart Grid.*, vol. 11, no. 2, pp. 1566–1581, 2020.

[9] J. W. Shim, G. Verbic, N. Zhang, and K. Hur, "Harmonious Integration of Faster-Acting Energy Storage Systems Into Frequency Control Reserves in Power Grid With High Renewable Generation," *IEEE Trans. Power Syst.*, vol. 33, no. 6, pp. 6193–6205, 2018.

[10] C. Mu, Y. Zhang, H. Jia, and H. He, "Energy-storage-based intelligent frequency control of microgrid with stochastic model uncertainties," *IEEE Trans. Smart Grid.*, vol. 11, no. 2, pp. 1748–1758, 2020.

[11] Y. Wang, Y. Xu, Y. Tang, K. Liao, MH. Syed, and E. Guillo-Sansano, and GM. Burt, "Aggregated energy storage for power system frequency control: a finite-time consensus approach," *IEEE Trans. Smart Grid.*, vol. 10, no. 4, pp. 3675–3686, 2019.

[12] S. Oshnoei et al. "A novel virtual inertia control strategy for frequency regulation of islanded microgrid using two-layer multiple model predictive control" *Applied Energy*, vol. 343, pp. 121233, Aug. 2023.

[13] A. Oshnoei et al. "Coordinated control scheme for provision of frequency regulation service by virtual power plants" *Applied Energy*, vol. 325, no. 1, pp. 119734, Nov. 2022.

[14] J. Pahasa, and I. Ngamroo, "PHEVs bidirectional charging/discharging and SoC control for microgrid frequency stabilization using multiple MPC," *IEEE Trans. Smart Grid.*, vol. 6, no. 2, pp. 526–533, 2015.

[15] A. Oshnoei, M. Kheradmandi, and S. M. Muyeen, "Robust control scheme for distributed battery energy storage systems in load frequency control," *IEEE Trans. Power Syst.*, vol 35, no. 6, pp. 4781-4791, 2020.

[16] H. Sorouri et al. ""An intelligent adaptive control of dc–dc power buck converters," *Int. J. Electr. Power Energy Syst.*, vol. 141, p. 108099, 2022.